Biophysical Chemistry 137 (2008) 95–99

Contents lists available at ScienceDirect

Biophysical Chemistry

journal homepage: http://www.elsevier.com/locate/biophyschem

Conformational stability and integrity of α-amylase from mung beans: Evidence of kinetic intermediate in GdmCl-induced unfolding

Pallavi Tripathi [a,b], Hagen Hofmann [b], Arvind M. Kayastha [a,*], Renate Ulbrich-Hofmann [b,*]

[a] School of Biotechnology, Faculty of Science, Banaras Hindu University, Varanasi-221005, India
[b] Institute of Biotechnology, Martin-Luther University, Kurt-Mothes Straße 3, D-06120 Halle, Germany

ARTICLE INFO

Article history:
Received 17 March 2008
Received in revised form 16 July 2008
Accepted 24 July 2008
Available online 30 July 2008

Keywords:
Protein folding
Thermal transitions
Unfolding kinetics
α-Amylase
Vigna radiata

ABSTRACT

α-Amylase from mung beans (*Vigna radiata*) being one of the few plant α-amylases purified so far was studied with respect to its conformational stability by CD and fluorescence spectroscopy. The enzyme was shown to bind 3–4 Ca^{2+} ions, which all are important for its activity. In contrast to other α-amylases no inhibition was observed at high Ca^{2+} concentrations (100 mM). Depletion of calcium decreased the transition temperature from 87 to 48 °C. Kinetic stopped-flow fluorescence measurements allowed detecting two unfolding phases at >6 M GdmCl, whereas only one phase was observed at <5 M GdmCl. These results suggest that the first (reversible) step of unfolding is slower than the second (irreversible) step at low GdmCl concentrations, whereas the rates of these two steps are opposite at high GdmCl concentrations.

Among starch hydrolyzing enzymes that are produced on an industrial scale, α-amylases (EC.3.2.1.1; 1,4-α-D glucan glucanohydrolase) are of considerable interest. In addition to their use in starch liquefaction for the production of glucose and maltodextrines, they are used in brewing, baking, paper and detergent industries. In general α-amylases are classified based on their sequence into family-13 of glycoside hydrolases [1]. α-Amylases occur in mammals, microorganisms and plants. They hydrolyse starch, glycogen and related polysaccharides by cleaving internal α-1,4 glucosidic bonds to produce maltooligosaccharides and glucose. Most α-amylase consists of a single polypeptide chain folded into three domains (A, B and C). The catalytic domain A consists of $(\beta/\alpha)_8$-barrel. Domains B and C are located roughly at opposite sides of this TIM-barrel. Domain B is probably responsible for the differences in substrate specificity and stability among the α-amylases [2]. Domain C constitutes the C-terminal part of the sequence and contains a Greek key motif and its functional role is yet to be established [3]. The presence of a calcium ion, which is located at the interface between the A and B domains, is conserved in all α-amylases with known three dimensional structures [4,5]. One or more additional calcium ions have been found in several structures. It has been suggested that the role of the calcium ions is mainly structural [6] and the conserved regions are involved in the architecture of the Ca^{2+} binding site and of the active site. The essential role of Ca^{2+} has been explained by the observation that its ligands belong to domains A and B, and a resulting ionic bridge between the two domains appears to stabilize the active site cleft [7]. A hyperthermophilic α-amylase with a novel (Ca, Zn) two metal centre has also been reported and it does not require the addition of metal ions for its full activity [8]. Many X-ray crystal structures have been reported in case of α-amylase such as *Aspergillus oryzae* TAKA α-amylase at 3 Å resolution [9] and 2.1 Å [10], porcine pancreas α-amylase (PPA) [11], *Aspergillus niger* α-amylase [4,12], barley α-amylase isozyme 2 (AMY2) [13], barley α-amylase isozyme 1 [14], and α-amylase from *Alteromonas haloplanctis* [15]. From stability studies it has been concluded that most α-amylases unfold irreversibly with one preceding reversible unfolding step [16]. An exception seems to be α-amylase from *A. haloplanctis* that exhibits a remarkable degree of reversibility [17].

Despite the great attention dedicated to α-amylases, there has been only limited information on α-amylases from plants. Particularly, the stability of these enzymes has been scarcely considered hitherto. We report here on the thermal and guanidium hydrochloride (GdmCl) induced unfolding of α-amylase from mung beans (*Vigna radiata*) (VrAMY), which has been recently purified and characterized [18]. Concluded from homology-modeling studies, this enzyme, possessing

Abbreviations: VrAMY, *Vigna radiata* α-amylase; AMY 1, barley α-amylase 1; AMY 2, barley α-amylase 2; BAA, *Bacillus amyloliquefaciens* α-amylase; BLA, *Bacillus licheniformis* α-amylase; PPA, porcine pancreatic amylase; GdmCl, Guanidine hydrochloride; DTT, Dithiothreitol; EDTA, Ethylenediaminetetraacetic acid; BSA, Bovine Serum Albumin.

* Corresponding authors. Kayastha is to be contacted at Tel.: +91 542 2368331; fax: +91 542 2368693. Ulbrich-Hofmann, Tel.: +49 345 5524864; fax: +49 345 5527303.
E-mail addresses: kayasthabhu@gmail.com (A.M. Kayastha), renate.ulbrich-hofmann@biochemtech.uni-halle.de (R. Ulbrich-Hofmann).

0301-4622/$ – see front matter © 2008 Elsevier B.V. All rights reserved.
doi:10.1016/j.bpc.2008.07.007

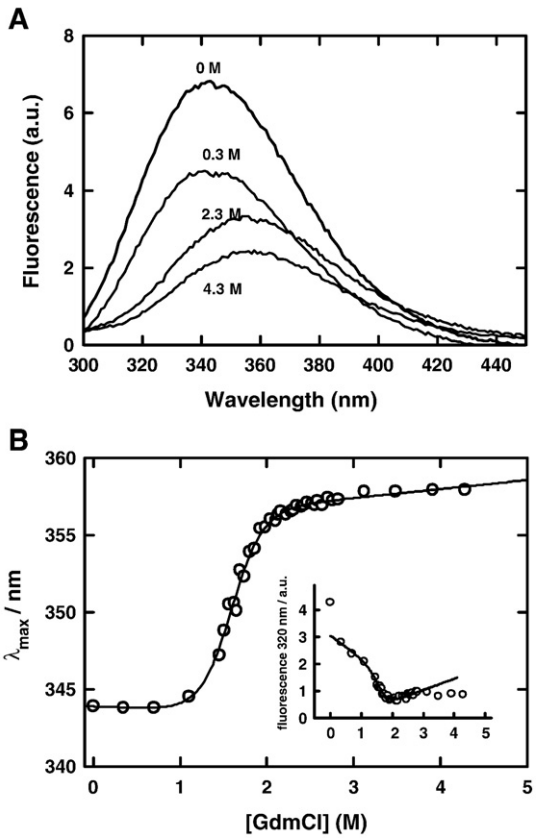

Fig. 1. GdmCl-induced unfolding. Fluorescence spectra of VrAMY (10 μg/ml) in 50 mM sodium acetate buffer, pH 5.5, containing 5 mM $CaCl_2$ and 1 mM DTT and different concentrations of GdmCl were taken at an excitation wavelength of 280 nm (A). The transition curve was constructed from the wavelength shift of the fluorescence maximum. Inset shows the transition curve plotted by intensities versus GdmCl concentrations (B).

70 and 73% sequence identity with the two α-amylases isoenzymes from barley (AMY1 and AMY2), has a similar tertiary structure as these enzymes but lacks two tryptophan residues which are conserved in other plant α-amylases and are assigned to the starch granule binding surface [14].

1. Materials and methods

1.1. Enzyme and other chemicals

VrAMY was purified according to Tripathi et al. [18], from the seeds of mung beans (*V. radiata*). For spectroscopic studies, buffer used was 50 mM sodium acetate, pH 5.5, containing 5 mM $CaCl_2$ and 1 mM DTT. EDTA, BSA and GdmCl (spectroscopic grade) were purchased from Sigma Chemical Co., St. Louis, MO, USA. Soluble starch, all buffers and other chemicals were from E. Merck and BDH Chemicals, India. All solutions were prepared in Milli Q (Millipore, Bedford, MA, USA) water.

1.2. Enzyme and protein assays

The activity of VrAMY was measured by the method of Fuwa [19]. The reaction mixture, containing 0.5 ml of 1% starch, 0.3 ml of 0.1 mol/l sodium acetate buffer (pH 5.5) and 0.1 ml of Milli Q water, was incubated at 55 °C for 10 min for equilibration. The reaction was started by the addition of 0.1 ml (suitably diluted) of enzyme solution and allowed to proceed for 5 min. The reaction was stopped by the addition of 0.5 ml of 1 mol/l HCl and cooled rapidly to room temperature. 0.2 ml of this reaction mixture was added to 15 ml Milli Q water and further, 0.1 ml of 1 mol/l HCl and 0.1 ml iodine reagent (0.2% iodine in 2.0% KI) was added to it for color development. A blank was prepared by adding the enzyme solution after the reaction has been stopped by the addition of HCl. The absorbance was measured at 610 nm on an Ultrospec 3000 UV spectrophotometer (Amersham Biosciences, Uppsala, Sweden). One unit of α-amylase was defined as the amount of enzyme, which caused a decrease of absorbance by 0.05 in starch iodine color under the assay conditions.

Protein was determined by the method of Bradford [20] with crystalline bovine serum albumin as the standard protein.

1.3. Effect of $CaCl_2$ and EDTA on enzyme activity

VrAMY (10 μg/ml) was incubated with different concentrations of $CaCl_2$ (0.5 mM–100 mM) at 25 °C overnight and assayed for amylolytic activity as described above. Then in the same samples 10 mM EDTA was added and incubated for 4 h, after the incubation period samples were assayed for the activity. For EDTA titration experiment, firstly the enzyme was dialyzed against the extraction buffer without $CaCl_2$ (50 mM sodium acetate, pH 5.5, 1 mM DTT) to ensure the removal of any external source of $CaCl_2$. Then different concentrations of EDTA (from 1 μM–400 mM) were added and samples were incubated for 4 h. Enzyme was then assayed for amylolytic activity. To check the reversibility of the activity lost after the addition of 10 mm EDTA, 10 mM $CaCl_2$ was added to the enzyme sample and activity was assayed after different time intervals till 4 h.

1.4. Circular dichroism (CD)

CD spectra in the far UV region (200–250 nm) were recorded on a JASCO J-810 spectrometer (Jasco, Gross-Umstadt, Germany) equipped with a Peltier thermostating cuvette holder using a constant nitrogen flow. VrAMY (0.15 mg/ml) was dissolved in 50 mM sodium acetate, pH 5.5, containing 5 mM $CaCl_2$ and 1 mM DTT. The spectra were recorded in a 1 mm cell at 20 °C at a scan speed of 200 nm/min with a residual

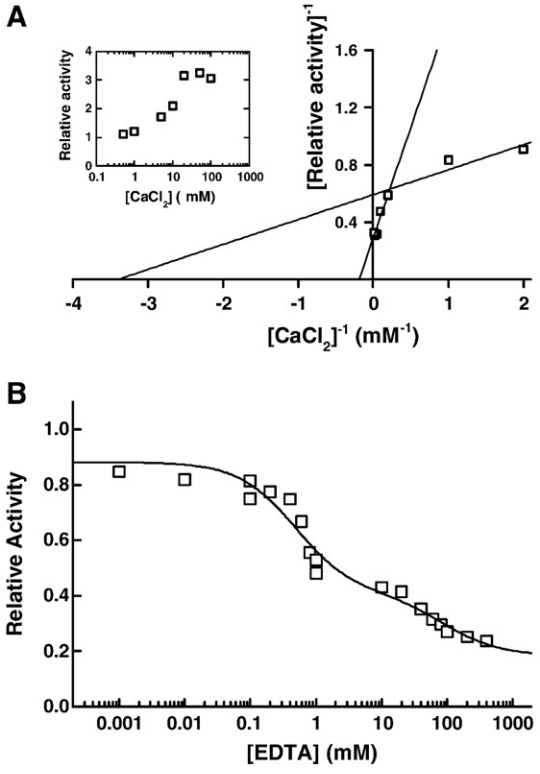

Fig. 2. Effect of Ca^{2+} ions (A) and EDTA (B) on activity. Protein concentration was 10 μg/ml. Buffer used was 50 mM sodium acetate buffer, pH 5.5, containing 5 mM $CaCl_2$ and 1 mM DTT, at 20 °C, dialysis was carried out against the same buffer without $CaCl_2$.

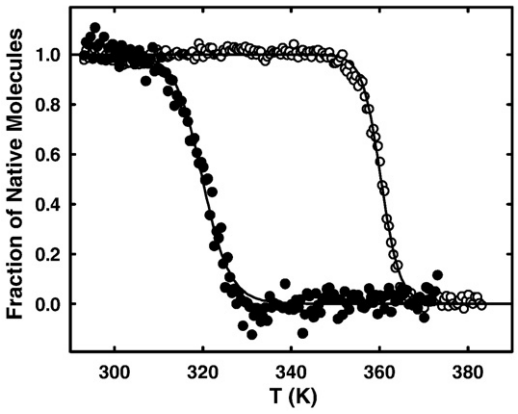

Fig. 3. Temperature induced unfolding. Thermal unfolding of VrAMY (0.15 mg/ml) in 50 mM sodium acetate buffer, pH 5.5, containing 5 mM $CaCl_2$ and 1 mM DTT (○) or 10 mM EDTA (●) was measured by CD spectroscopy. The intensity of the signal at 222 nm was followed as function of temperatures (30–115 °C) at a heating rate of 1 °C/min.

time of 15 s and a bandwidth of 1 nm. Three scans were averaged and corrected for the buffer signal.

Thermal transitions were monitored by measuring the CD signal of VrAMY (0.15 mg/ml) in the absence and presence of 10 mM EDTA at 222 nm at different temperatures (30–115 °C) with a heating rate of 1 °C/min.

1.5. Fluorescence spectroscopy

Intrinsic fluorescence was measured by Fluoromax 2, Jovin Yvon-Spex Instrument Inc., U.S.A. Excitation wavelength in general was 280 nm and emission spectra were recorded in the range between 300 and 450 nm. All fluorescence emission spectra were corrected for background scattering as measured with pure buffer. All spectra were recorded at 20 °C and corrected for buffer. Protein concentration was 10 μg/ml, buffer used was 50 mM sodium acetate, pH 5.5, containing 5 mM $CaCl_2$ and 1 mM DTT.

1.6. Unfolding kinetics with manual mixing

Enzyme solutions were placed in the flourimeter Fluoromax 2 and buffer solution containing pre-calculated concentrations of GdmCl were rapidly added with constant stirring. Final protein concentration in the sample was 10 μg/ml. Fluorescence intensity at 343 nm was followed as function of time. The excitation wavelength was 280 nm. The dead time of this procedure was about 10 s. The kinetics were measured in 50 mM sodium acetate buffer, pH 5.5, containing 5 mM $CaCl_2$ and 1 mM DTT, at 20 °C.

1.7. Unfolding kinetics with stopped-flow mixing

Stopped-flow fluorescence kinetics was performed on an Applied Photophysics SX-20MV stopped-flow instrument at 20 °C. An excitation wavelength of 280 nm was used and the fluorescence above 320 nm was collected. Unfolding experiments were performed by mixing the enzyme and buffer containing pre-calculated concentrations of GdmCl, to 1:11 ratio. The final enzyme concentration was 20 μg/ml.

2. Results

2.1. Far-UV CD and fluorescence spectra

The CD spectrum of VrAMY showed two minima at 208 nm and 222 nm, typical of α-helical proteins. Secondary structure analysis of the CD spectra by the online program K2D [21,22] estimated α helix 31%, β sheet 15% and random coils 54%.

The fluorescence spectrum of native VrAMY (Fig. 1A) showed maximum emission intensity at 343 nm, indicating a hydrophobic environment for tryptophan residues.

2.2. The effect of calcium ions on activity

The incubation of enzyme samples, having various $CaCl_2$ concentration (from 0.5 mM–100 mM), with 10 mM EDTA for 4 h, resulted in a remarkable activation of VrAMY (Fig. 2A). From the double-reciprocal plot (Fig. 2A) of the activity data as function of the $CaCl_2$ concentration, two apparent dissociation constants could be estimated, $K_1 = 0.3 \pm 0.1$ mM and $K_2 = 5.4 \pm 1.0$ mM.

The addition of EDTA to VrAMY, dialyzed before to remove any metal ions from the solution, led to a distinct decrease of enzyme activity. From the semi-logarithmic plot of the activity data *vs.* the EDTA concentration (Fig. 2B), the presence of at least one, probably two additional Ca^{2+}-binding sites could be derived. The activity lost by EDTA (10 mM, incubation for 4 h) could not be regained after the addition of excess $CaCl_2$, demonstrating the irreversibility of inactivation.

2.3. Thermal transition

The thermal unfolding of VrAMY was observed by CD measurements in the presence of 5 mM $CaCl_2$ or 10 mM EDTA at an enzyme concentration of 0.15 mg/ml. The resulting transition curves taken at a heating rate of 1 °C/min (Fig. 3) reflect cooperative unfolding processes in both cases but with strong differences in the transition

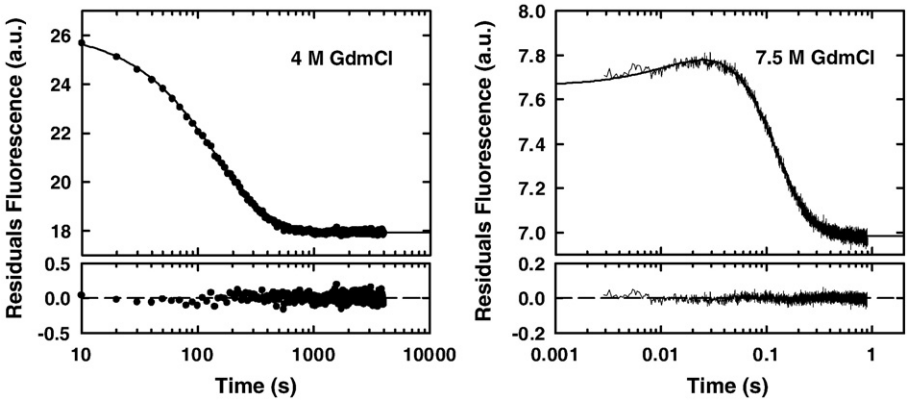

Fig. 4. Unfolding kinetics in GdmCl. The fluorescence signal of VrAMY (10 μg/ml) in 50 mM sodium acetate buffer, pH 5.5, containing 5 mM $CaCl_2$ and 1 mM DTT was recorded after manual or stopped-flow mixing with 4 or 7.5 M GdmCl as described in Materials and methods.

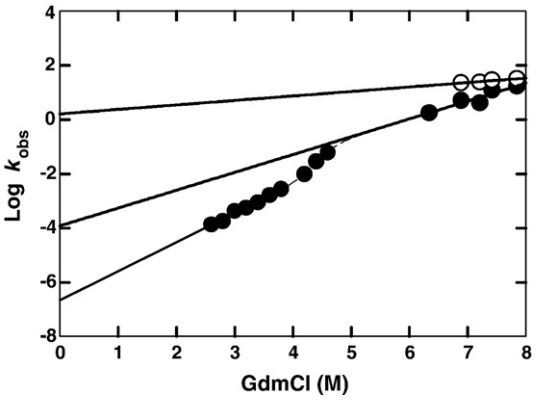

Fig. 5. Half-Chevron plot representing the unfolding kinetics rate constants plotted as the function of different GdmCl concentrations. The rate constants k_{obs} for the unfolding of VrAMY (10 μg/ml for manual mixing and 20 μg/ml for stopped-flow mixing) in 50 mM sodium acetate buffer, pH 5.5, containing 5 mM $CaCl_2$ and 1 mM DTT were determined from the unfolding kinetics as exemplified in this figure. The constants were calculated by single (2.8–4.6 M GdmCl) or double (6.3–7.8 M GdmCl) exponential fits. Open and closed circles represent the rate constants for fast and slow unfolding reactions, respectively.

temperature $T_{1/2}$, which was 87 °C in the presence of 5 mM $CaCl_2$ and 48 °C in the presence of 10 mM EDTA. These results indicate that the stability of the protein is severely compromised in absence of calcium ions.

2.4. GdmCl-induced transition

Fluorescence spectra of VrAMY were taken in the presence of increasing concentrations of GdmCl after overnight preincubation in this denaturant. As exemplified in Fig. 1A the emission maximum of VrAMY shifted toward longer wavelengths and the signal intensity decreased. In 4.3 M GdmCl, the emission maximum reached 356 nm, which indicates an extensive protein unfolding [23,24].

From the red-shift of the fluorescence maxima and the decrease of the fluorescence intensities (Fig. 1A), transition curves were constructed, which provide the picture of a cooperative two-state transition (Fig. 1B). The $[GdmCl]_{1/2}$ values, indicating the denaturant concentration where half of the protein molecules are unfolded, are in good accordance when calculated from the wave-length shift (1.59 ± 0.02 M) or signal intensity (1.63 ± 0.06 M).

2.5. GdmCl-induced unfolding kinetics

To obtain information on the unfolding pathway resulting in irreversibility of VrAMY, unfolding kinetics was followed at GdmCl concentrations in the range of 2.8–7.8 M by measuring the fluorescence signal at 343 nm. To detect fast unfolding phases (in the millisecond range) stopped-flow mixing experiments were included additional to the experiments with manual mixing. While the unfolding at low GdmCl concentrations (<5 M) was slow and only one unfolding phase could be found, the measurement of unfolding at high GdmCl concentrations (>6 M) demanded stopped-flow mixing and two phases were detectable. As exemplified in Fig. 4 for 4 and 7.5 M GdmCl, the unfolding kinetics of VrAMY at 2.8–4.6 M GdmCl could be fitted by a first-order reaction, whereas at 6.3–7.8 M GdmCl a double-exponential fit was necessary. The rate constants resulting from these fits were plotted as function of the GdmCl concentration (Half-Chevron plot) in Fig. 5.

3. Discussion

While the stability and unfolding of mammalian and microbial α-amylases have been intensively investigated [16,25], there have been only a few studies on the conformational stability of plant α-amylases, namely of the two isoenzymes from barley AMY1 and AMY2 [26,27]. The present studies aimed at first insights into the stability of VrAMY, in comparison with the corresponding properties of the related AMY1 and AMY2 (with 70 and 73% identity in the amino acid sequences) as well as bacterial and mammalian α-amylases as far as known from literature.

The CD and fluorescence (Fig. 1) spectra of the native enzyme were similar to those of the barley isoenzymes [26] or also from *B. amyloliquefaciens* [24]. Even α-amylase from the psychrophile bacterium *A. haloplanctis* shows a related CD spectrum [28] reflecting the common type of the TIM-barrel structure, which is characteristic of the family 13 of glycosyl hydrolase.

One of the main characteristic features of α-amylases studied so far is their requirement of Ca^{2+} ions for activity and structural stability. Beside one essential Ca^{2+} ion, in most α-amylases localized between domains A and B [4,7], additional stabilizing Ca^{2+} ions are suggested. As reviewed by Fitter [25], TAKA amylase binds two Ca^{2+} ions, the α-amylases from *Bacillus subtilis* and *Bacillus licheniformis* are able to bind three Ca^{2+} ions and the enzyme from *Bacillus amyloliquefaciens* is characterized by four binding sites for Ca^{2+} ions. In contrast, only one Ca^{2+} binding site was assured for PPA and for α-amylase from the psychrophile *A. haloplanctis*. The two barley enzymes AMY1 and AMY2 contain at least one Ca^{2+} ion each [26]. According to Robert et al. [14], three or even four Ca^{2+} ions can be bound by these enzymes. Our activity studies on VrAMY (Fig. 2) also suggest 3–4 binding sites for Ca^{2+} ions. As can be concluded from the inactivation of VrAMY by EDTA (Fig. 2B), one or two Ca^{2+} ions are strongly bound to the enzyme with affinity differences of about one order of magnitude. As in case of the barley isoenzymes and several bacterial α-amylases [26,29,30], this inactivation is irreversible and suggests an essential function of the metal ion in stabilizing the active site structure. From the activation of VrAMY by Ca^{2+} ions (Fig. 2A), two low-affinity binding sites for Ca^{2+} ions with dissociation constants in the millimolar range (0.3 and 5.4 mM) can be derived. Therefore, it seems that plant α-amylases show a similar variety in Ca^{2+} binding sites as microbial α-amylases. An inactivation at higher concentrations of Ca^{2+} ions as reported for AMY1 and AMY2 [14] was not observed with VrAMY.

As in other α-amylases the main function of the Ca^{2+} ions consists in structural stabilization as demonstrated in thermal unfolding of VrAMY in the presence of 5 mM $CaCl_2$ compared to Ca^{2+}-depleted enzyme (Fig. 3). Both in the presence and absence of Ca^{2+} ions, VrAMY undergoes a cooperative conformational transition with a difference of the $T_{1/2}$ values of 39 K. This stabilization effect by Ca^{2+} ions is similar as that observed in microbial α-amylases as reviewed in [31], while these effects have not yet been studied for other plant α-amylases. Because of the irreversibility of thermal transitions and different experimental conditions, $T_{1/2}$ values can only roughly be compared with literature data of other α-amylases. In such a comparison, VrAMY (at 5 mM $CaCl_2$) with a $T_{1/2}$ value of 87 °C proved to be more stable than AMY1 and AMY2 which showed $T_{1/2}$ values of 78 and 80.5 °C [27].

A general scheme of irreversible denaturation has been proposed:

$$N \rightleftarrows U \rightarrow D \quad (1)$$

where N stands for native protein, U stands for unfolded protein and D stands for denatured protein, a reversible conformational change is assumed to precede the irreversible step (aggregation, misfolding, covalent modification). Our trials to refold the enzyme after different interval of unfolding had failed. So, most probably the "unfolding reaction" is coupled to an aggregation process or is itself aggregation. It is physically unreasonable to assume that the native molecules directly aggregate in GdmCl. Hence, an additional state (unfolded or intermediate) was introduced to account for the possibility of an aggregation process. The two phases observed in the unfolding experiments at high GdmCl concentrations give a hint for the two successive processes. To analyze this process for α-amylases, most authors measured the thermal irreversible inactivation kinetics [30,32–34]. From first-order kinetics they concluded that the first

(unfolding) step is rate limiting and connected with the release of Ca^{2+} ions, which makes the molecule prone to fast aggregation. Our studies on GdmCl-induced unfolding of VrAMY (Fig. 1) showed a cooperative transition without any indication of intermediates in the unfolding process. Similar curves were observed for AMY1 and AMY2 [27]. A careful kinetic analysis, however, combining manual with stopped-flow mixing techniques in fluorescence spectroscopy, revealed kinetic differences dependent on the concentration range of the denaturant. While only one (slow) unfolding step could be observed at low GdmCl concentrations (Figs. 4 and 5), two processes with rates differing by about one order of magnitude could be differentiated at >6 M GdmCl (Figs. 4 and 5). From these data it can be concluded that the first step is rate limiting at low GdmCl concentrations, whereas with increasing GdmCl concentrations the rate of the first step increases until the second irreversible step becomes rate limiting. These measurements allowed to quantify the rates of the two reaction steps in irreversible unfolding of α-amylases for the first time and might be the basis for further mechanistic analyses of the irreversibility of enzyme inactivation processes.

In summary, the results show that VrAMY, the only plant α-amylase in addition to the two well-characterized isoenzymes from barley, behaves similar to the most microbial and mammalian α-amylases but shows also some individual characteristics which might be interesting for potential industrial applications. The kinetic differentiation of two unfolding steps opens the way to a better understanding of the irreversible unfolding of multi-domain proteins.

Acknowledgements

Financial assistance of the Council of Scientific and Industrial Research (CSIR), New Delhi (Senior Research Fellowship to PT) is thankfully acknowledged. PT would also like to thank DAAD (Sandwich Model Fellowship), Germany for funding to carry out a part of research work in Germany.

References

[1] B. Henrissat, A classification of glycosyl hydrolases based on amino acid sequence similarities, Biochem. J. 280 (1991) 309–316.
[2] B. Svensson, Protein engineering in the α-amylase family: catalytic mechanism, substrate specificity, and stability, Plant Mol. Biol. 25 (1994) 141–157.
[3] P.K. Nielsen, B.C. Bonsager, K. Fukuda, B. Svensson, Barley α-amylase/subtilisin inhibitor: structure, biophysics and protein engineering, Biochim. Biophys. Acta. 1696 (2004) 157–164.
[4] E. Boel, R.L. Brady, A.M. Brzozowski, Z.S. Derewenda, G.G. Dodson, V.J. Jensen, S.B. Petersen, H. Swift, L. Thim, H.F. Woldike, Calcium binding in α-amylases: an X-ray diffraction study at 2.1-Å resolution of two enzymes from *Aspergillus*, Biochemistry 29 (1990) 6244–6249.
[5] M. Machius, G. Wiegand, R. Huber, Crystal structure of calcium-depleted *Bacillus licheniformis* α-amylase at 2.2 Å resolution, J. Mol. Biol. 246 (1995) 545–559.
[6] C. Gilles, J.P. Astier, G. Marchis-Mouren, C. Cambillau, F. Payan, Crystal structure of pig pancreatic α-amylase isoenzyme II, in complex with the carbohydrate inhibitor acarbose, Eur. J. Biochem. 238 (1996) 561–569.
[7] G. Buisson, E. Duee, R. Haser, F. Payan, Three-dimensional structure of porcine pancreatic α-amylase at 2.9 Å resolution. Role of calcium in structure and activity, EMBO. J. 6 (1987) 3909–3916.
[8] A. Linden, O. Mayans, W. Meyer-Klaucke, G. Antranikian, M. Wilmanns, Differential regulation of a hyperthermophilic α-amylase with a novel (Ca, Zn). Two metal center by zinc, J. Biol. Chem. 278 (2003) 9875–9884.
[9] Y. Matsuura, M. Kusunoki, W. Harada, M. Kakudo, Structure and possible catalytic residues of Taka-amylase A, J. Biochem. (Tokyo) 95 (1984) 697–702.
[10] H.J. Swift, L. Brady, Z.S. Derewenda, E.J. Dodson, G.G. Dodson, J.P. Turkenburg, A.J. Wilkinson, Structure and molecular model refinement of *Aspergillus oryzae* (TAKA) α-amylase: an application of the stimulated-annealing method, Acta Crystallogr. B. 47 (1991) 535–544.
[11] M. Qian, R. Haser, F. Payan, Structure and molecular model refinement of pig pancreatic α-amylase at 2.1 Å resolution, J. Mol. Biol. 231 (1993) 785–799.
[12] R.L. Brady, A.M. Brzozowski, Z.S. Derewenda, E.J. Dodson, G.G. Dodson, Solution of the structure of *Aspergillus niger* acid α-amylase by combined molecular replacement and multiple isomorphous replacement methods, Acta Crystall. B. 47 (1991) 527–535.
[13] A. Kadziola, J. Abe, B. Svensson, R. Haser, Crystal and molecular structure of barley α-amylase, J. Mol. Biol. 231 (1994) 104–121.
[14] X. Robert, R. Haser, T.E. Gottschalk, B. Svensson, N. Aghajari, The structure of barley α-amylase isozyme 1 reveals a novel role of domain C in substrate recognition and binding: a pair of sugar tongs, Structure 11 (2003) 973–984.
[15] N. Aghajari, G. Feller, C. Gerday, R. Haser, Crystal structures of the psychrophilic α-amylase from *Alteromonas haloplanctis* in its native form and complexed with an inhibitor, Protein Sci. 7 (1998) 564–572.
[16] J.E. Nielsen, T.V. Borchert, Protein engineering of bacterial α-amylases, Biochim. Biophys. Acta 1543 (2000) 253–274.
[17] G. Feller, D. d`Amico, C. Gerady, Thermodynamic stability of a cold-active alpha-amylase from the Antarctic bacterium *Alteromonas haloplanctis*, Biochemistry 38 (1999) 4613–4619.
[18] P. Tripathi, L.L. Leggio, J. Mansfeld, R.U. Hofmann, A.M. Kayastha, α-Amylase from mung beans (*Vigna radiata*) — correlation of biochemical properties and tertiary structure by homology modeling, Phytochemistry 68 (2007) 1623–1631.
[19] H. Fuwa, A new method for microdetermination of amylase activity by the use of amylose as the substrate, J. Biochem. (Tokyo) 41 (1954) 583–603.
[20] M. Bradford, A rapid and sensitive method for the quantitation of microgram quantities of protein utilizing the principle of protein-dye binding, Anal. Biochem. 72 (1976) 248–254.
[21] M.A. Andrade, P. Chacón, J.J. Merelo, F. Morán, Evaluation of secondary structure of proteins from UV circular dichroism using an unsupervised learning neural network, Prot. Eng. 6 (1993) 383–390.
[22] J.J. Merelo, M.A. Andrade, A. Prieto, F. Morán, Proteinotopic feature maps, Neurocomputing 6 (1994) 443–454.
[23] F.X. Schmid, Optical spectroscopy to characterize protein conformation and conformational changes, in: T.E. Creighton (Ed.), Protein structure, A Practical Approach, Ed. 2nd, Oxford University Press Inc., New York, 1997, pp. 261–296.
[24] J. Fitter, S. Haber-Pohlmeier, Structural stabilities and unfolding properties of thermostable bacterial α-amylases: a comparative study on homologous enzymes, Biochemistry 43 (2004) 9589–9599.
[25] J. Fitter, Structural and dynamical features contributing to thermostability in alpha-amylases, Cell. Mol. Life Sci. 62 (2005) 1925–1937.
[26] D.S. Bush, L. Sticher, R. van Huystee, D. Wagner, R.L. Jones, The calcium requirement for stability and enzymatic activity of two isoforms of barley aleurone α-amylase, J. Biol. Chem. 264 (1989) 19392–19398.
[27] M.T. Jensen, T.E. Gottschalk, B. Svensson, Differences in conformational stability of barley alpha-amylase isozymes 1 and 2. Role of charged groups and isozyme 2 specific salt bridges, J. Cereal Sci. 38 (2003) 289–300.
[28] G. Feller, S. D'Amico, A.M. Benotmane, F. Joly, J. Van Beeumen, C. Gerday, Characterization of C-terminal propeptide involved in bacterial wall spanning of alpha-amylase from the psychrophile *Altermonas haloplnactis*, J. Biol. Chem. 273 (1998) 12109–12115.
[29] D.N. Lecker, A. Khan, Theoretical and experimental studies of the effects of heat, EDTA and enzyme concentration on the inactivation rate of α-amylase from *Bacillus* sp, Biotechnol. Prog. 12 (1996) 713–717.
[30] A. Tanaka, E. Hoshino, Diffusion characteristics of substrates in Ca-alginate gel beads, Biochem. J. 364 (2002) 635–639.
[31] C. Duy, J. Fitter, Thermostability of irreversible unfolding alpha-amylases analyzed by unfolding kinetics, J. Biol. Chem. 280 (2005) 37360–37365.
[32] (a). S.J. Tomazic, A.M. Klibanov, Mechanisms of irreversible thermal inactivation of *Bacillus* α-amylases, J. Biol. Chem. 263 (1988) 3086–3091;
(b). S.J. Tomazic, A.M. Klibanov, Why is *Bacillus* alpha-amylase more resistant against irreversible thermoinactivation than another? J. Biol. Chem. 263 (1988) 3092–3096.
[33] M. Violet, J.C. Meunier, Kinetic study of the irreversible thermal denaturation of *Bacillus licheniformis* alpha-amylase, Biochem. J. 263 (1989) 665–670.
[34] N. Declerck, M. Machius, P. Joyet, G. Wiegand, R. Huber, C. Gaillardin, Hyperthermostablilization of *Bacillus licheniformis* α-amylase and modulation of its stability over a 50 °C temperature range, Protein Eng. 16 (2003) 287–293.